Electronic Supplementary Information

Crack healing and reclaiming of vulcanized rubber by triggering rearrangement of inherent sulfur crosslinked networks

Hong Ping Xiang,[a] Hu Jun Qian,[b] Zhong Yuan Lu,[b] Min Zhi Rong*[a] and Ming Qiu Zhang*[a]

[a] *Key Laboratory for Polymeric Composite and Functional Materials of Ministry of Education, GD HPPC Lab, School of Chemistry and Chemical Engineering, Sun Yat-sen University, Guangzhou 510275, P. R. China. E-mail:* cesrmz@mail.sysu.edu.cn and ceszmq@mail.sysu.edu.cn.

[b] *State Key Laboratory of Theoretical and Computational Chemistry, Institute of Theoretical Chemistry, Jilin University, Changchun 130023, China*

Determination of equilibrium constant and kinetic parameter of model disulfide metathesis

For the following disulfide metathesis in equilibrium, A-S-S-A + B-S-S-B $\rightleftharpoons$ A-S-S-B, the equilibrium constant, K_{eq}, was calculated from:

$$K_{eq} = \frac{[\mathrm{A-S-S-B}]_{eq}^2}{[\mathrm{A-S-S-A}]_{eq}[\mathrm{B-S-S-B}]_{eq}}$$

where $[\mathrm{A\text{-}S\text{-}S\text{-}A}]_{eq}$ and $[\mathrm{B\text{-}S\text{-}S\text{-}B}]_{eq}$ denote equilibrium concentrations of reactants A-S-S-A and B-S-S-B, while $[\mathrm{A\text{-}S\text{-}S\text{-}B}]_{eq}$ denotes equilibrium concentration of product A-S-S-B.

Supposing disulfide metathesis follows the first- or second-order kinetics:

$$\ln\left(\frac{1}{1-x}\right) = kt \qquad \text{(first order kinetics)}$$

$$\frac{1}{1-x} = kt \qquad \text{(second order kinetics)}$$

where x is conversion, k rate constant and t reaction time. Linear fit of the data offers rate constant at a given temperature. Finally, activation energy, E_a, can be calculated from Arrhenius equation based on the relationship between k and T:

$$k = Ae^{-E_a/\mathrm{RT}}$$

Determination of densities of sulfur crosslinks[S1-S4]

To determine the percentage of sulfur crosslinks in the total number of crosslinks of vulcanized rubber, selective scission of specific crosslinks in association with crosslinking density

measurement was applied. Firstly, the vulcanizate was treated with 0.4*M* propanethiol in piperidine at 25 ºC for 6 h to cleave only the polysulfidic crosslinks. Then, the cosslinking density of the treated vulcanizate was measured by equilibrium swelling method (see below). Comparison of the crosslinking densities of the vulcanizate before and after the treatment allowed the calculation of the contribution of polysulfidic crosslinks to the total degree of crosslinks. Similarly, the concentration of both polysulfide and disulfide crosslinks was estimated by treating the vulcanizate with 1*M* 1-hexanethiol in piperidine at 25 ºC for 48 h to cleave polysulfide and disulfide crosslinks. As a result, the individual contribution of disulfide crosslinks was obtained by subtracting the concentration of polysulfidic crosslinks from that of polysulfide and disulfide crosslinks.

To measure crosslinking density, vulcanized samples (~0.5 g) were immersed in toluene to swell at 25 ºC for 72 h. The swollen samples were weighed after removal of surface liquid with filter paper. Then the swollen samples were dried at 80 ºC in vacuum to constant weight and weighed again. The crosslinking density per unit volume, ν, was calculated from Flory-Rehner equation:

$$\nu = \frac{\nu_r + \chi\nu_r^2 + \ln(1-\nu_r)}{\nu_s(0.5\nu_r - \nu_r^{1/3})}$$

$$\nu_r = \frac{m_r}{m_r + m_s\dfrac{\rho_r}{\rho_s}}$$

where ν_r is the volume fraction of rubber in the swollen sample, ν_s is the molar volume of the solvent, m_r is the weight of the rubber network after drying, m_s is the weight of solvent absorbed at equilibrium, ρ_r is the density of rubber, ρ_s is the density of solvent, χ is the Flory-Huggins interaction parameter for polybutadiene rubber-toluene system taken as a constant (0.36). On the basis of the crosslinking densities, concentration of polysulfide crosslinks, $S_x\%\ (x>2)$, and total concentration of polysulfide and disulfide crosslinks, $S_{x1}\%\ (x\geq 2)$, can be known by:

$$S_x\%(x>2) = \frac{\nu - \nu_t}{\nu} \times 100\%$$

$$S_x\%(x\geq 2) = \frac{\nu - \nu_{t1}}{\nu} \times 100\%$$

where v is the crosslink density of the virgin sample, v_t is the crosslink density of the sample treated by propanethiol, v_{t1} is the crosslink density of the sample treated by hexanethiol.

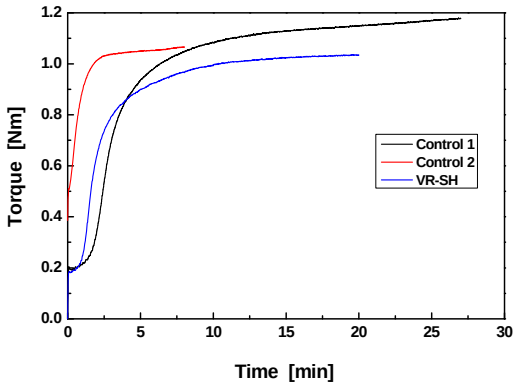

Fig. S1 Rheographs of the rubbers cured at 150 ºC. The characteristic t_{90}, the optimum vulcanization time required for reaching specific torque value which is the sum of minimum torque and 90 % of the differentials between maximum and minimum torque.

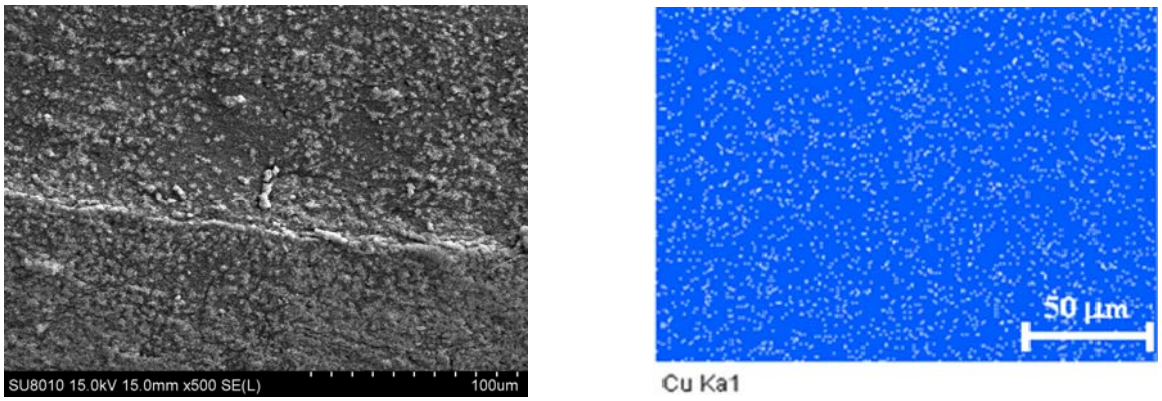

(a) (b)

Fig. S2 (a) Scanning electron microscopic (SEM) micrograph of typical fractured surface of $CuCl_2$/polybutadiene rubber ($CuCl_2$ content = 1 phr), which was compounded under the same conditions as VR-SH. (b) Energy dispersive spectroscopy (EDS) image of typical fractured surface of VR-SH using copper as the indicator element.

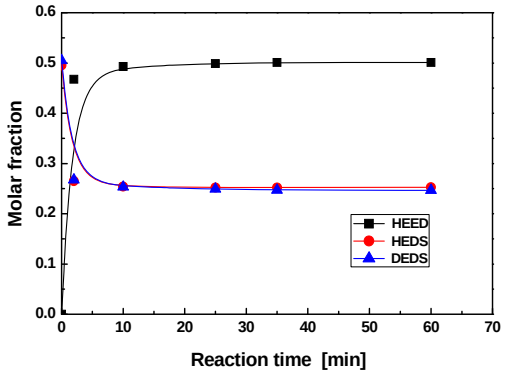

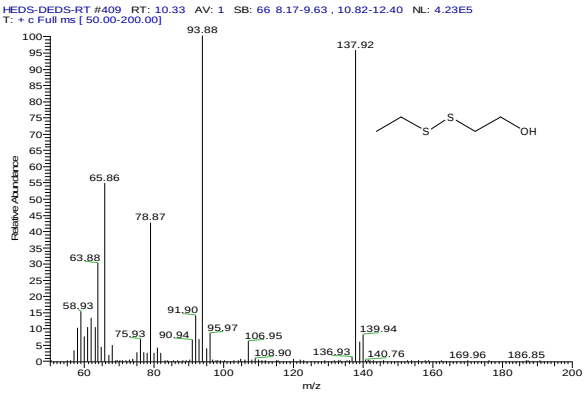

(a) (b)

Fig. S3 (a) Time dependences of molar fractions of the disulfides in equimolar mixture of HEDS and DEDS determined from HLPC chromatograms in **Fig. 1** (25 ºC, acetonitrile, 0.5 mol% $CuCl_2$). (b) Mass spectrum of the metathesis product HEED. The signal at m/z ≈ 138 is a molecular ion peak, just half of the sum of m/z ≈ 154 (HEDS) and half of m/z ≈ 122 (DEDS). The ion peaks at m/z ≈ 94, 79 and 66 belong to the fragments of -S-S-C_2H_5, -S-S-CH_2, and -S-S-, respectively.

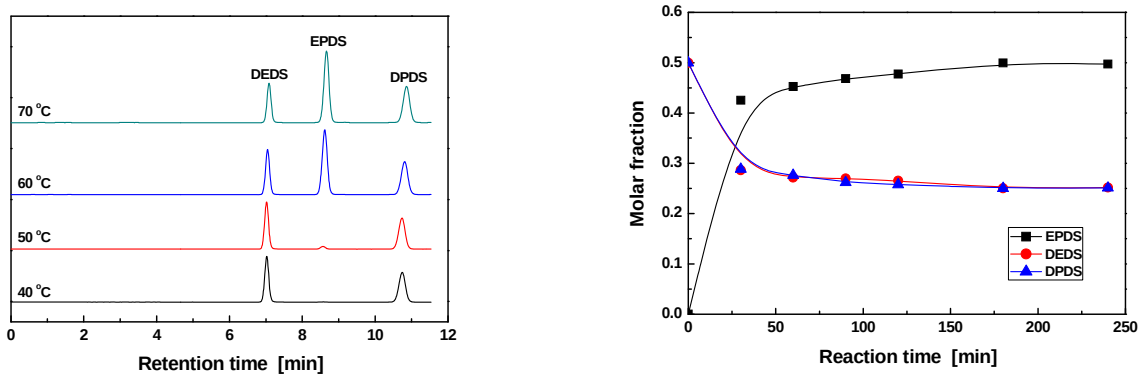

(a) (b)

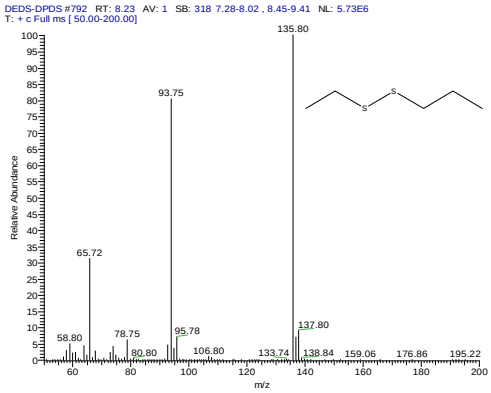

(c)

Fig. S4 (a) HLPC analysis of equimolar mixture of DPDS and DEDS collected at different temperatures (3 h, *n*-heptane, 0.5 mol% $CuCl_2$). Here, DPDS replaces HEDS used in (**Fig. 1**) because the latter does not dissolve in *n*-heptane. (b) Time dependences of molar fractions of the disulfides in equimolar mixture of DPDS and DEDS determined from HLPC chromatograms at 70 ºC. (c) Mass spectrum of the metathesis product ethyl propyl disulfide (EPDS).

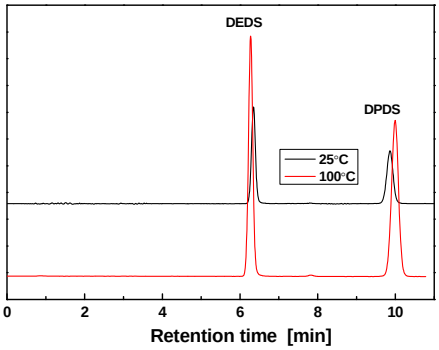

Fig. S5 HPLC analysis of equimolar mixture of DEDS and DPDS in acetonitrile at 25 ºC for 5 h and in *n*-heptane 100 ºC for 1 h.

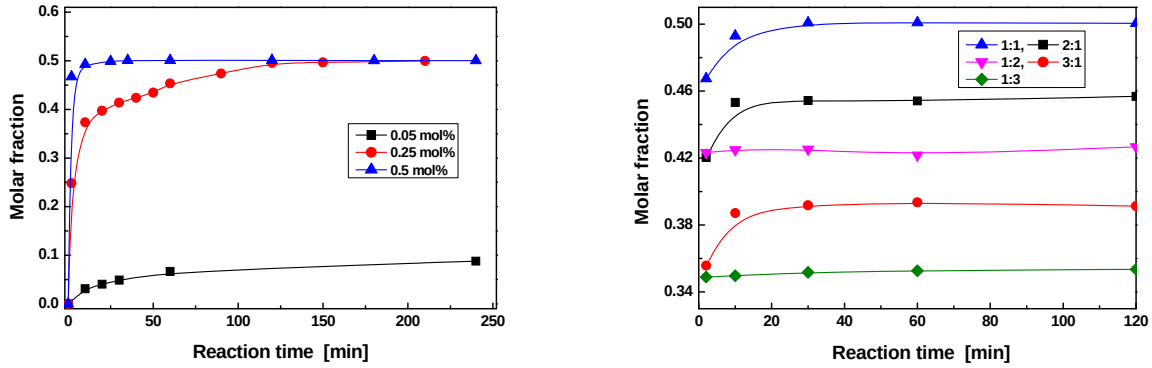

(a) (b)

Fig. S6 Time dependences of molar fractions of HEED produced from disulfide metathesis between HEDS and DEDS at 25 ºC in acetonitrile. (a) Effect of $CuCl_2$ dosage on conversion of equimolar HEDS and DEDS. (b) Effect of initial molar ratio of HEDS to DEDS on conversion ($CuCl_2$: 0.5 mol%).

Table S1. Effect of initial molar ratio of reactants on K_{eq} in acetonitrile at 25 ºC *

$[HEDS]_o$:$[DEDS]_o$	$[HEDS]_o$	$[DEDS]_o$	$[HEDS]_{eq}$	$[DEDS]_{eq}$	$[HEED]_{eq}$	K_{eq}
1:1	100	100	49.94	50.05	100	4.00
2:1	133.33	66.67	82.37	26.26	91.37	3.86
3:1	150	50	106.66	14.90	78.39	3.87
1:2	66.67	133.33	20.52	94.44	85.05	3.73
1:3	50	150	11.34	117.95	70.73	3.74

*$[HEDS]_o$ and $[DEDS]_o$ are initial concentrations of HEDS and DEDS. $[HEDS]_{eq}$, $[DEDS]_{eq}$ and $[HEED]_{eq}$ are equilibrium concentrations of HEDS, DEDS and HEED. Unit of the concentrations: mmol L^{-1}. Content of $CuCl_2$: 0.50 mol%.

Table S2. Effect of temperature on K_{eq} in acetonitrile*

T (ºC)	$[HEDS]_o$	$[DEDS]_o$	$[HEDS]_{eq}$	$[DEDS]_{eq}$	$[HEED]_{eq}$	K_{eq}
0	100	100	49.47	50.69	99.96	3.99
-10	100	100	60.52	60.74	78.88	1.69
-15	100	100	63.98	67.64	68.31	1.08
-20	100	100	69.78	70.18	59.87	0.73
-30	100	100	77.94	79.02	43.07	0.30

*Content of $CuCl_2$: 0.50 mol%.

Table S3. Effect of dosage of $CuCl_2$ on K_{eq} in acetonitrile at 25 ºC

Dosage (mol %)	$[HEDS]_o$	$[DEDS]_o$	$[HEDS]_{eq}$	$[DEDS]_{eq}$	$[HEED]_{eq}$	K_{eq}
1.25	100	100	49.41	50.66	99.82	3.98
0.50	100	100	49.94	50.05	100	4.00

Table S4. Effect of temperature on K_{eq} in *n*-heptane*

T (ºC)	$[DPDS]_o$	$[DEDS]_o$	$[DPDS]_{eq}$	$[DEDS]_{eq}$	$[EPDS]_{eq}$	K_{eq}
50	100	100	88.14	94.04	17.82	0.04
53	100	100	80.36	85.69	34.02	0.17
55	100	100	75.75	76.48	47.80	0.39
60	100	100	50.05	50.07	99.96	3.99

*Content of $CuCl_2$: 0.50 mol%.

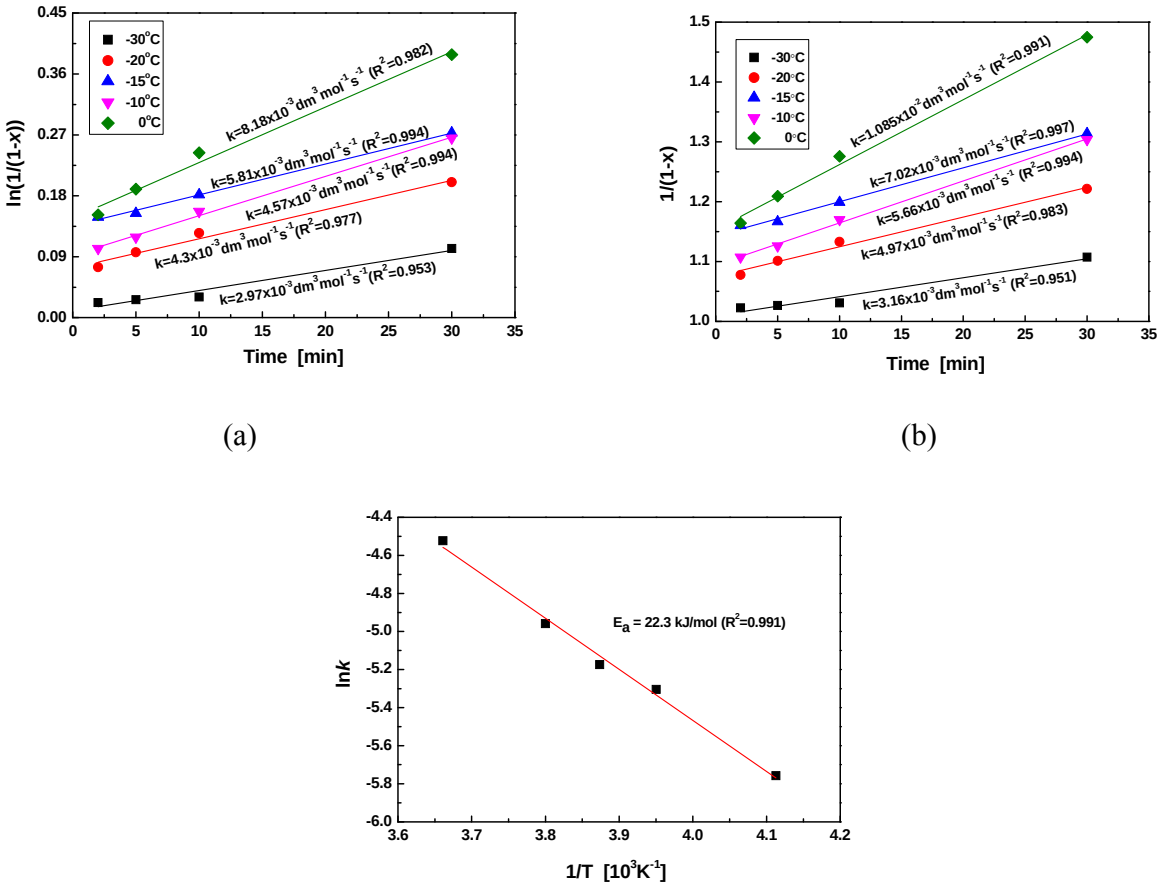

(a) (b)

(c)

Fig. S7 Linear regression of conversion, *x*, versus time, *t*, of disulfide metathesis between HEDS and DEDS with 0.5 mol% $CuCl_2$ in acetonitrile according to (a) first-order and (b) second-order kinetics. The higher regression coefficients of the plots in (b) suggest that the second-order kinetics reaction should be more reasonable. Therefore, the activation energy is estimated using *k* values provided by the second-order kinetics.

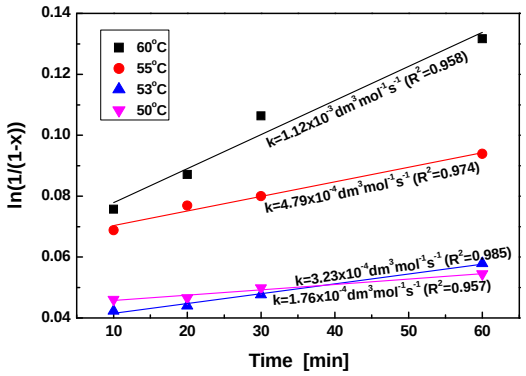

(a)

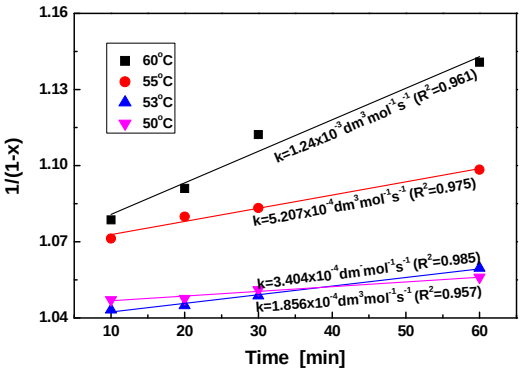

(b)

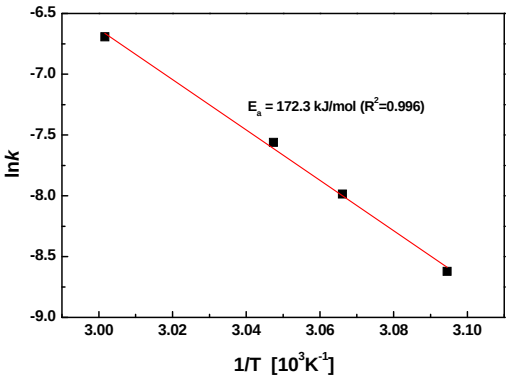

(c)

Fig. S8 Linear regression of conversion, *x*, versus time, *t*, of disulfide metathesis between DEDS and DPDS with 0.5 mol% $CuCl_2$ in *n*-heptane according to (a) first-order and (b) second-order kinetics. The higher regression coefficients of the plots in (b) suggest that the second-order kinetics reaction should be more reasonable. Therefore, the activation energy is estimated using *k* values provided by the second-order kinetics.

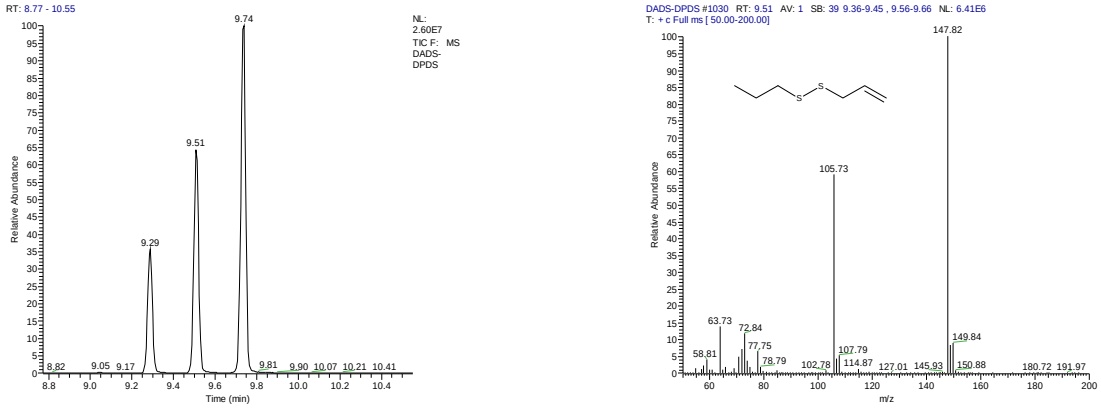

(a) (b)

Fig. S9 GC-MS analyses of the metathesis between DADS and DPDS with 0.5 mol% $CuCl_2$ in *n*-heptane at 70 ºC for 3 h. (a) Gas chromatograph of the reaction system, and (b) mass spectrum of the metathesis product. The peak at 9.51 min is assigned to be allyl propyl disulfide, because the molecular ion peak (m/z ≈ 148) is just half of the sum of DPDS (m/z ≈ 150) and DADS (m/z ≈ 146).

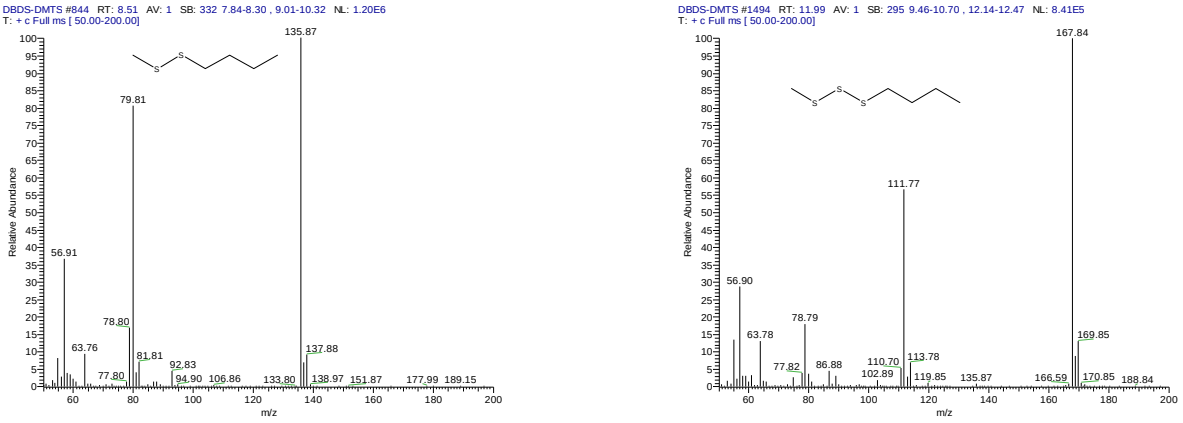

(a) (b)

Fig. S10 Mass spectra of the metathesis products between DBDS and DMTS with 0.5 mol% $CuCl_2$ in *n*-heptane at 70 ºC for 3 h. Because scission of DMTS would offer two species (CH_3-S- and CH_3-S-S-) to react with DBDS at the same time, two metathesis products appear, i.e. (a) methyl butyl disulfide (m/z ≈ 136) and (b) methyl butyl trisulfide (m/z ≈ 168).

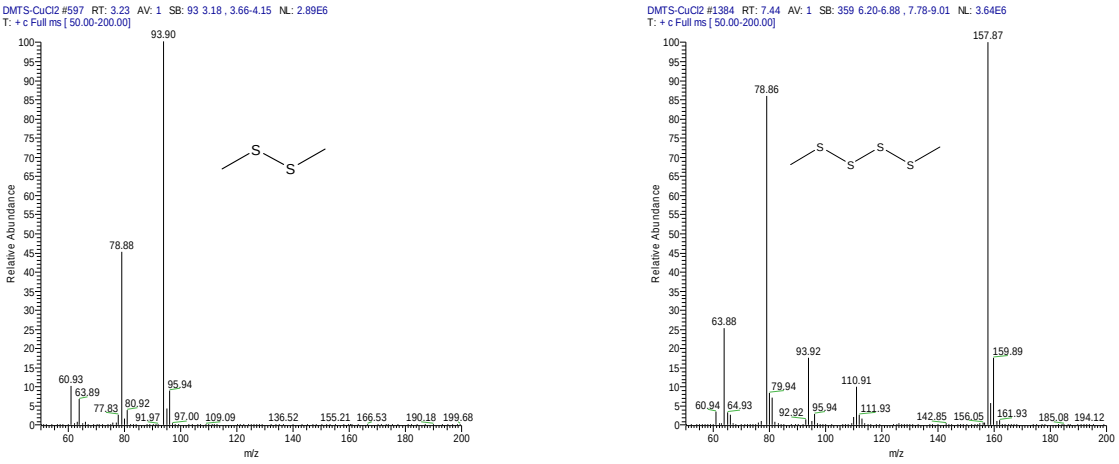

(a) (b)

Fig. S11 Mass spectra of the metathesis products of DMTS with 0.5 mol% $CuCl_2$ in acetonitrile at 25 ºC for 1 h. (a) Dimethyl disulfide (m/z ≈ 94) and (b) dimethyl tetrasulfide (m/z ≈ 158).

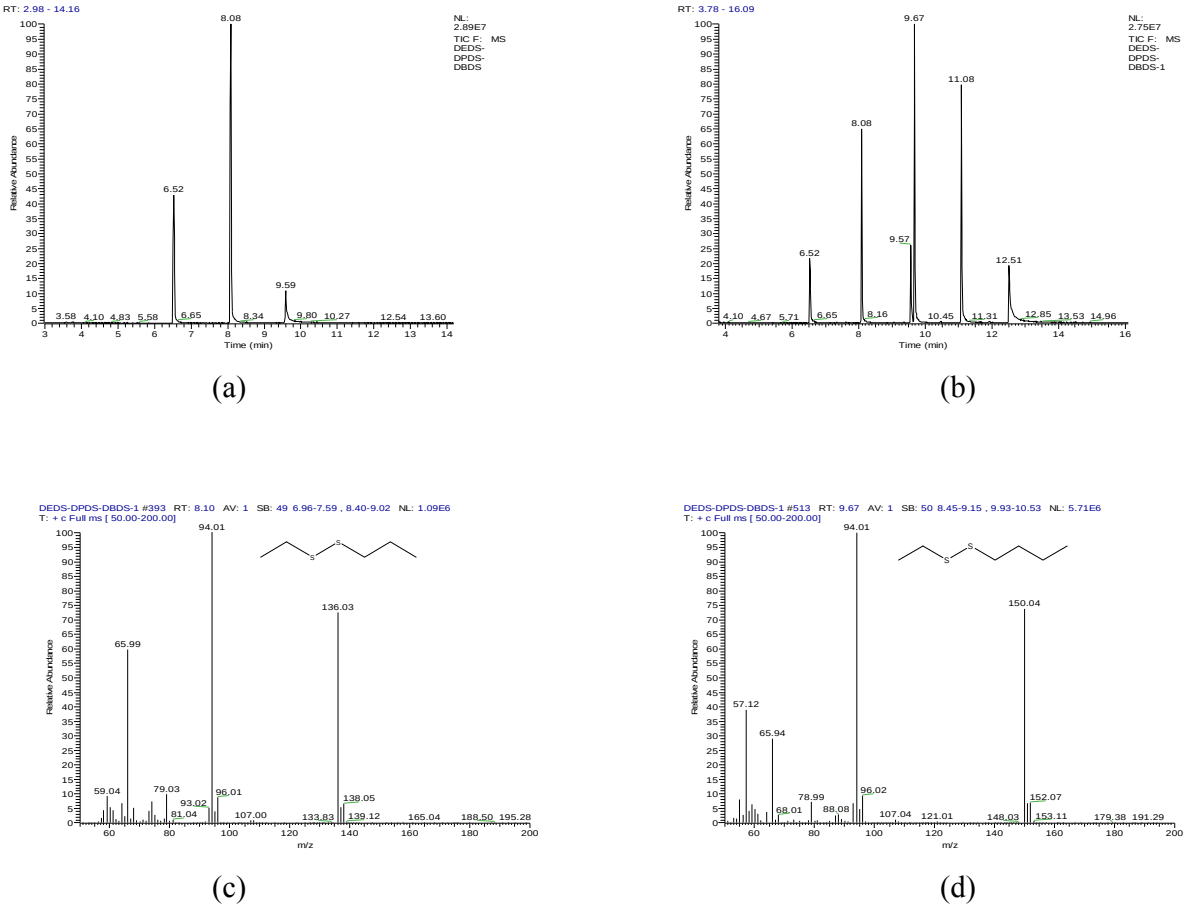

(c) (d)

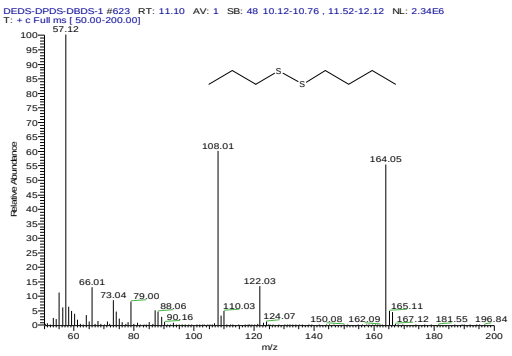

(e)

Fig. S12 Dynamic reversibility of disulfide metathesis in acetonitrile catalyzed by 0.5 mol% $CuCl_2$ at 25 ºC. (a) Gas chromatograph of metathesis between DEDS and DPDS in equilibrium. (b) Gas chromatograph of metathesis among DEDS, DPDS and DBDS in equilibrium. Equimolar DBDS was added when the metathesis between DEDS and DPDS had reached the equilibrium. (c) Mass spectrum of the metathesis product (ethyl propyl disulfide (EPDS)) between DEDS and DPDS. (d) Mass spectrum of the metathesis product (ethyl butyl disulfide (EBDS)) between DEDS and DBDS. (e) Mass spectrum of the metathesis product (propyl butyl disulfide (PBDS)) between DPDS and DBDS. The ratios of DEDS:EPDS:DPDS:EBDS:PBDS:DBDS attained from the normalized peak areas are 11:21:12:23:22:12, near the statistical values.

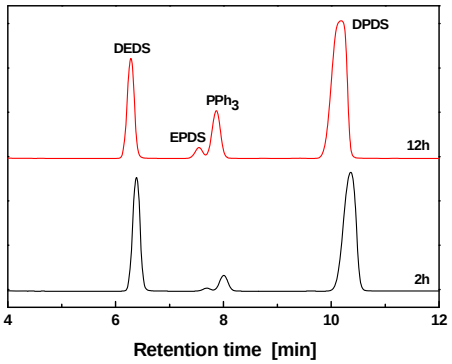

Fig. S13 HLPC analysis of disulfide metathesis between equimolar HEDS and DEDS at 100 ºC catalyzed by 1 mol% PPh_3. Because of the high evaporation rate of acetonitrile and *n*-heptane at 100 ºC, the reaction proceeded in the absence of any solvent.

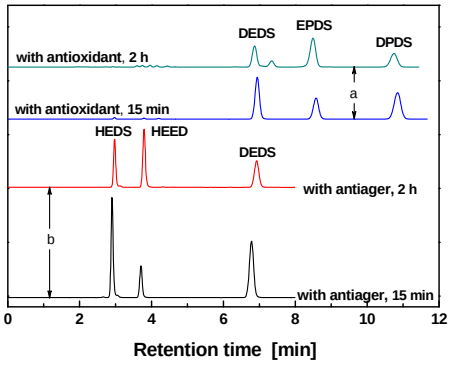

Fig. S14 HLPC analysis of disulfide metathesis between (a) equimolar DEDS and DPDS in the presence of 5 mol% antioxidant tris(2,4-di-tert-butylphenyl)phosphate, and (b) equimolar HEDS and DEDS in the presence of 5 mol% antiager poly(1,2-dihydro-2,2,4-trimethyl-quinoline). The reactions are carried out in acetonitrile at 25 ºC with 0.5 mol% $CuCl_2$.

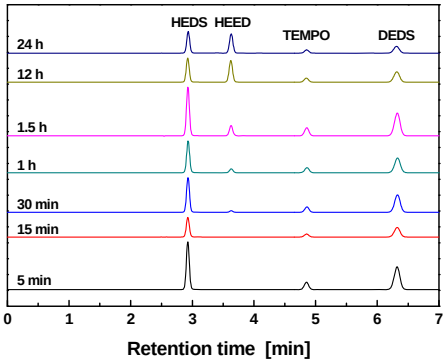

(a)

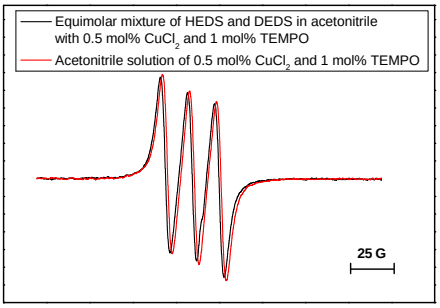

(b)

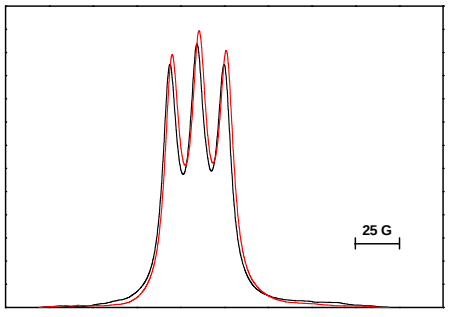

(c)

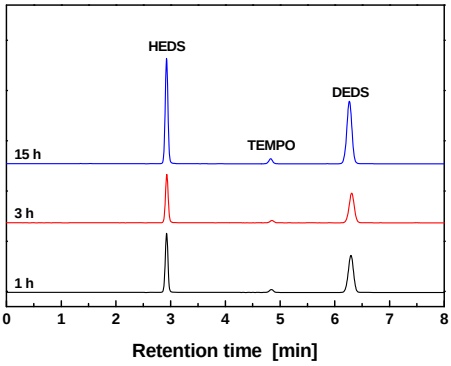

(d)

Fig. S15 (a) HLPC analysis of disulfide metathesis between equimolar of HEDS and DEDS in acetonitrile with 0.5 mol% $CuCl_2$ and 1 mol% TEMPO at 25 ºC. All the chemicals are mixed at

the same time. (b) ESR spectrum of the reaction system in (a) collected at 24 h in comparison with that of a reference system, which has the same compositions as (a) but the disulfide mixtures are replaced by isopycnic acetonitrile. (c) Integration of (b). (d) HLPC analysis of the reaction system having the same components as (a), but $CuCl_2$ and TEMPO are firstly mixed in acetonitrile under stirring for 30 min prior to the addition of acetonitrile solution of HEDS and DEDS.

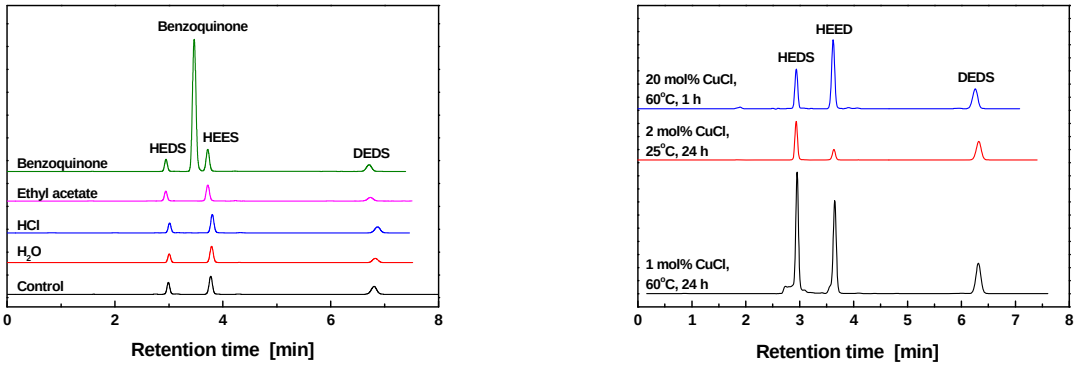

(a) (b)

Fig. S16 (a) Effect of different inhibitors (10 mol %) on disulfide metathesis between equimolar HEDS and DEDS in acetonitrile for 30 min with 0.5 mol% $CuCl_2$ at 25 ºC. (b) HLPC analysis of disulfide metathesis between equimolar HEDS and DEDS in acetonitrile catalyzed by CuCl under different conditions.

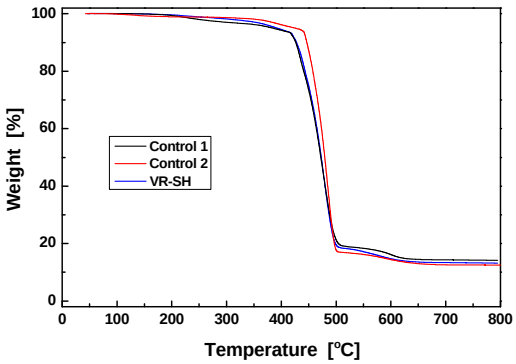

Fig. S17 Thermal decomposition behaviors of the cured rubbers.

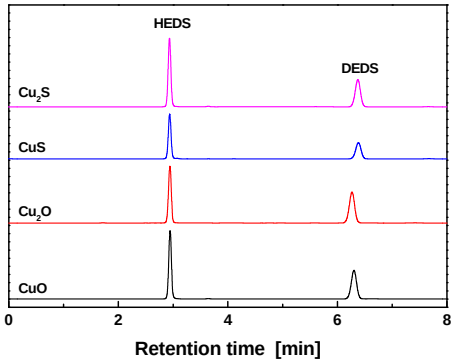

Fig. S18 HLPC analysis of disulfide metathesis between equimolar HEDS and DEDS in acetonitrile at 60 ºC for 24 h catalyzed by 5 mol% Cu_2S, CuS, Cu_2O and CuO, respectively.

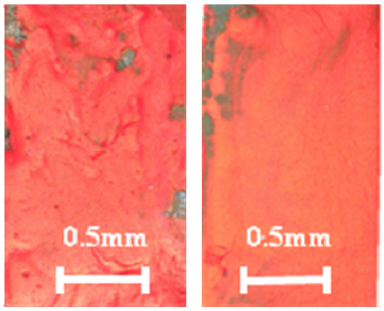

Fig. S19 Identification of non-contact regions on the combined fractured surfaces. Firstly, paired tensile fractured specimens were cooled down by liquid nitrogen. Then, one part of the pair was uniformly dyed with red oil paint. Finally, the dyed fragment was brought into contact with its undyed counterpart. When the two halves of the broken specimen were separated again, the unstained portions on the originally undyed fragment (refer to the photos shown above) represent the non-contact regions on the combined fractured surfaces.

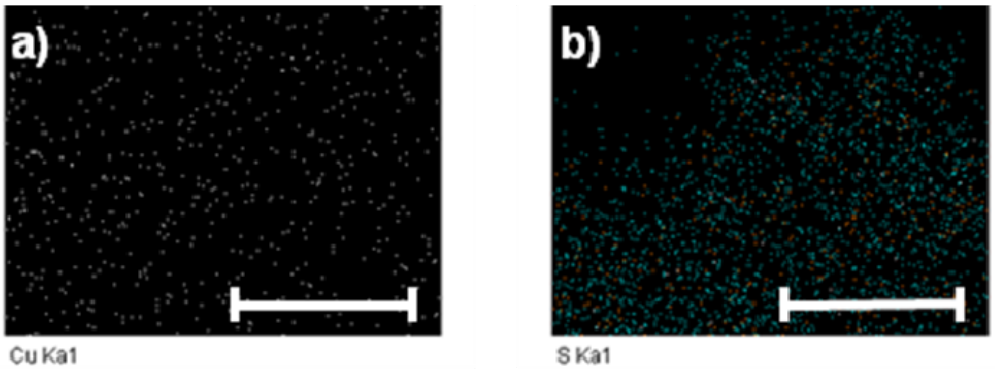

Fig. S20 EDS images of the fracture surface of control vulcanized rubber without Si-69 using a) copper and b) sulfur as the indicator elements. Here the vulcanized rubber has the same composition as VR-SH but excludes Si-69. The attached scale bars represent 1 mm in length.

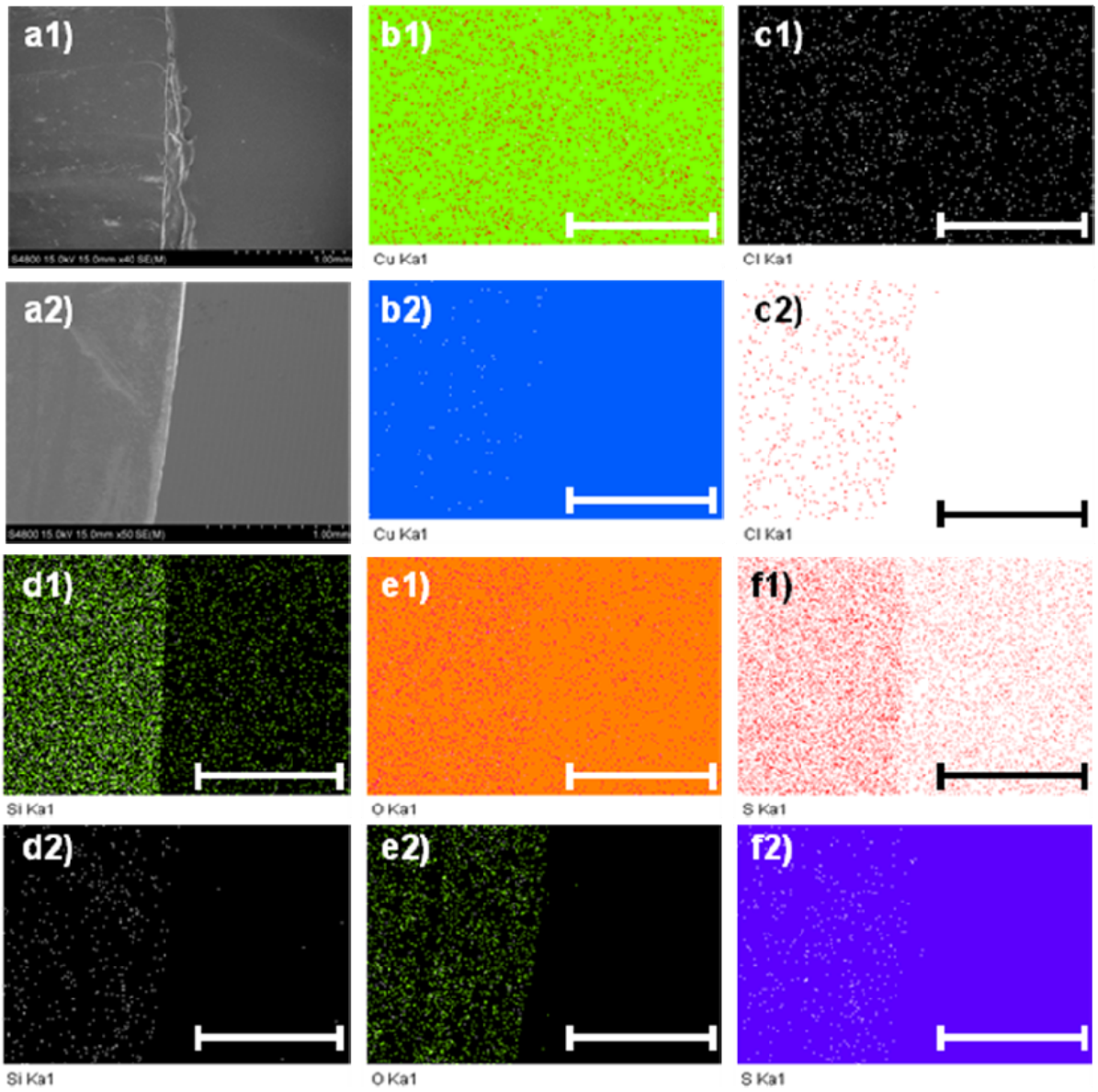

Fig. S21 Model experiment showing improved mobility of $CuCl_2$ with the help of Si-69. (a) SEM and (b-f) EDS images of side faces of two pieces of contacted rubbers (left: VR-SH; right: polybutadiene). The VR-SH in (a1-f1) contains Si-69, while that in (a2-f2) does not. The indicator elements of EDS images include (b) copper, (c) chlorine, (d) silicon, (e) oxygen, and (f) sulfur. After treatment at 110 ºC for 48 h, $CuCl_2$ successfully migrates from VR-SH to polybutadiene with the aid of Si-69, and is dispersed in the latter (refer to b1-f1). Comparatively, only a few $CuCl_2$ can migrate from VR-SH to polybutadiene because of lack of Si-69 (refer to b2-f2). The attached scale bars represent 1 mm in length.

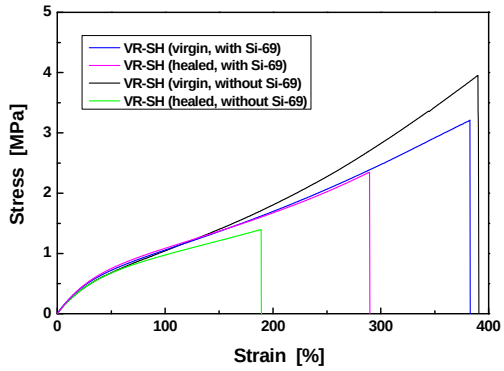

Fig. S22 Typical tensile stress-strain curves of virgin and healed VR-SH specimens in comparison with those of virgin and healed control vulcanized rubber without Si-69. Healing temperature: 110 ºC; healing time: 12 h.

Notes and references

S1 P. Posadas, A. Fernández, J. Brasero, J. L. Valentín, A. Marcos, A. Rodríguez and L. González, *J. Appl. Polym. Sci.*, 2007, **106**, 3481-3487.

S2 L. González, A. Rodríguez, A. Del Campo and A. Marcos-Fernández, *J. Appl. Polym. Sci*., 2002, **85**, 491-499.

S3 J. L. Valentín, A. Rodríguez, A. Marcos-Fernández and L. González, *J. Appl. Polym. Sci*., 2004, **93**, 1756-1761.

S4 R. L. Fan, Y. Zhang, F. Li, Y. X. Zhang, K. Sun and Y. Z. Fan, *Polym. Test*., 2001, **20**, 925-936.